


Article

Detection of Raspberry Ketone after Percutaneous Absorption of Rhododendrol-Containing Cosmetics and Its Mechanism of Formation

Lihao Gu ¹, Akio Fujisawa ^{1,2} and Kazuhisa Maeda ^{1,2,*} 

¹ Bionics Program, Tokyo University of Technology Graduate School, 1404-1 Katakura-machi, Hachioji City, Tokyo 192-0982, Japan; d1117001d4@edu.teu.ac.jp (L.G.); afujisawa@stf.teu.ac.jp (A.F.)

² School of Bioscience and Biotechnology, Tokyo University of Technology, 1404-1 Katakura-machi, Hachioji City, Tokyo 192-0982, Japan

* Correspondence: kmaeda@stf.teu.ac.jp; Tel.: +81-426372442

Abstract: Here, we aimed to elucidate the mechanism of rhododendrol (RD)-induced leukoderma. We investigated the skin permeability of RD in an aqueous solution and in different cosmetic formulations (lotion and emulsion) in an in vitro skin permeation study. The samples were analyzed using high-performance liquid chromatography (HPLC), and an unknown substance appeared on the spectrum. For identification, we analyzed various possible substances, such as raspberry ketone (RK) and rhododendrol quinone, using HPLC and then compared the detected absorption spectra and further verified the matched components using liquid chromatography–mass spectrometry. The unknown substance was found to be RK. To clarify the mechanism of formation of RK, we conducted a 24-h skin permeation test on heat-treated skin. By quantifying the RK in the samples using HPLC, we observed that an enzyme in the skin seemed to be the cause of RK generation and that the components of the emulsion formulation could also be a cause. To investigate the enzyme, we reacted alcohol dehydrogenase with RD and observed that it was one of the converting enzymes. As RK has been reported to be a substance that causes leukoderma, the intraepidermal metabolism of RD to RK may be one of the mechanisms of susceptibility to leukoderma.

Keywords: rhododendrol; raspberry ketone; susceptibility to leukoderma; alcohol dehydrogenase; cytotoxicity



Citation: Gu, L.; Fujisawa, A.; Maeda, K. Detection of Raspberry Ketone after Percutaneous Absorption of Rhododendrol-Containing Cosmetics and Its Mechanism of Formation. *Cosmetics* **2021**, *8*, 97. <https://doi.org/10.3390/cosmetics8040097>

Academic Editor: Antonio Vassallo

Received: 9 September 2021

Accepted: 8 October 2021

Published: 12 October 2021

Publisher's Note: MDPI stays neutral with regard to jurisdictional claims in published maps and institutional affiliations.



Copyright: © 2021 by the authors. Licensee MDPI, Basel, Switzerland. This article is an open access article distributed under the terms and conditions of the Creative Commons Attribution (CC BY) license (<https://creativecommons.org/licenses/by/4.0/>).

1. Introduction

Because bright skin looks cleaner, and for other reasons, East Asian countries have tried since ancient times to make their skin brighter. Presently, brightening cosmetics are becoming more popular. Epidermal depigmentation products, such as brightening cosmetics, are typed according to their modes of action, which include promoting the excretion of melanin, melanin breakdown, inhibiting melanocyte activity, and inhibiting melanin synthesis by inhibiting tyrosinase, a key enzyme in the melanosome formation pathway [1].

Among products that inhibit tyrosinase, cosmetics containing 2% 4-(p-hydroxyphenyl)-2-butanol or rhododendrol (RD), which was developed in 2008 as an active ingredient of quasi-drugs, were voluntarily recalled after leukoderma was confirmed in consumers who had used them. As of November 2016, there were 19,605 confirmed cases of leukoderma. Most of these patients have recovered, but some still suffer from the disease even after 3 years [2].

RD is a chemically synthesized product obtained via catalytic hydrogen reduction of 4-(p-hydroxyphenyl)-2-butanone or raspberry ketone (RK) using a Raney nickel catalyst (Figure 1). RD contains a mixture of (R)-RD and (S)-RD enantiomers. When it is absorbed into the human body, it is known that RD is easily oxidized to oxides such as

RD-quinone [3,4]. Although a detailed mechanism by which RD causes leukoderma has not yet been elucidated, the underlying mechanism of leukoderma pathogenesis appears to be the catalyst for melanocyte tyrosinase to generate o-quinone from phenolic compounds, resulting in oxidative stress and cell toxicity [3–7]. We have shown that the pathogenesis of RD-induced leukoderma is due to the generation of hydroxyl radicals from RD, catalyzed by tyrosinase in the melanosomes of melanocytes [8].



Figure 1. Reduction of raspberry ketone (RK) to rhododendrol (RD).

RK is a raw material for RD which itself causes leukoderma. A 1988 study of RK suggested a mechanism for this [9,10]. It was reported that the cytotoxicity of RK is enhanced by the presence of tyrosinase, suggesting that leukoderma caused by RK is not due to the inhibition of melanin biosynthesis but the formation of toxic substances from RK by tyrosinase and the resulting destruction of melanocytes [9]. Both RD and RK are phenols with a substituted 4-position. Many studies on leukoderma caused by 4-position-substituted phenols have been previously reported. For example, occupational leukoderma caused by 4-tert-butylphenol, 4-octylphenol, and other 4-substituted phenols has been reported to have occurred in resin, rubber, paint, and surfactant manufacturing plants since 1960 [11–17]. The structure of the chemicals that cause leukoderma is characteristic, especially for 4-substituted phenols with a hydroxylated 1-position of the benzene ring and alkyl groups with non-polar side chains at the 4-position.

Given that skin-whitening products with RD are applied multiple times a day, the concentration of RD in the skin has the potential to reach toxic levels. Therefore, determining the amount of RD that is transepidermally absorbed is critical. Moreover, as the onset of toxicity is known to differ between individuals, this phenomenon may vary depending on the metabolic activity of RD in the epidermis. Therefore, the purpose of this study was to clarify the conversion of RD to RK in the skin using the skin permeation test and to determine whether RK was also responsible for leukoderma caused by RD-containing cosmetics.

2. Materials and Methods

2.1. Materials

Glycerin was purchased from Sakamoto Yakuhin Kogyo Co., Ltd. (Osaka, Japan). PEG-60 hydrogenated castor oil (HCO-60) was purchased from Nippon Surfactant Industries Co., Ltd. (Tokyo, Japan). Squalene was purchased from Nikko Chemicals Co., Ltd. (Tokyo, Japan). Phenoxyethanol (PHE-S) was purchased from Yokkaichi Chemical Co., Ltd. (Mie, Japan). Sodium acrylate–sodium acryloyldimethyl taurate copolymer/iso-hexadecane/polysorbate 80 (SIMULGEL-EG) was purchased from SEPPIC SA (Courbevoie, France). RK was purchased from Sigma-Aldrich Co. LLC (St. Louis, MO, USA). RD was purchased from Tokyo Chemical Industry Co., Ltd. (Tokyo, Japan). A Franz diffusion cell was purchased from Biocom Systems, Inc. (Fukuoka, Japan). Laboskin (4 cm × 7 cm; frozen dorsal full-thickness skin from a Hos:HR-1 hairless mouse) was purchased from Hoshino Laboratory Animals Inc. (Ibaraki, Japan). Considering animal welfare, we used the minimum amount of laboskin necessary. Phosphate-buffered saline (PBS) was purchased from TaKaRa Bio Inc. (Shiga, Japan). Moreover, 1,3-butanediol, acetic acid, methanol, sodium pyrophosphate, NAD⁺, and alcohol dehydrogenase (ADH) from yeast with a specific activity of 390 international enzyme units per mg of protein were purchased from FUJIFILM Wako Pure Chemical Corporation (Osaka, Japan).

2.2. Preparation of the Test Solution

As shown in Table 1, three test solutions containing 2% RD (the concentration that is used in Kanebo Cosmetics and causes leukoderma) were prepared. Ultrasound (US-2R, AS ONE Corporation, Tokyo, Japan; high mode, 40–50 °C, 20 min) was used to ensure uniform dissolution. The pH of all three solutions was adjusted to 6.2 using a 1% potassium hydroxide solution.

Table 1. Test solutions with different cosmetic formulations.

	Water	Lotion	Emulsion
RD	0.2	0.2	0.2
Glycerin	-	0.4	0.4
1,3-butanediol	-	0.6	0.6
PEG-60 hydrogenated castor oil	-	0.02	0.02
Phenoxyethanol	-	0.035	0.035
Squalene	-	-	1
Sodium acrylate–sodium acryloyldimethyl taurate copolymer/ isohexadecane/polysorbate 80	-	-	0.25
Water	9.8	8.745	7.495

All measurements are in grams.

2.3. Measurement of Skin Permeability after Repeated Application of Solutions Containing RD

Laboskin from 7-week-old mice was thawed to room temperature and prepared into a circular shape with an area of approximately 1.5 cm² using surgical scissors. Experiments were conducted to determine the amount of skin penetration when the formulations were applied in the actual dosage form used. Specifically, laboskin was mounted in a Franz diffusion cell with circulating water at a constant temperature of 37 °C, and 15 mg of a 2% RD solution (2% RD, 98% water) was applied once to 1.5 cm² of laboskin, followed by a second application 10 min later and a third application 10 min later.

High-performance liquid chromatography (HPLC) was performed using a Shimadzu HPLC system (Shimadzu Co., Kyoto, Japan), Capcell Pak C18 columns (4.6 × 250 mm; Shiseido Co. Ltd., Tokyo, Japan) at 35 °C, and an SPD-M20A photo diode array detector (Shimadzu Co., Kyoto, Japan) with the following conditions: flow rate, 1.0 mL/min; injection volume, 10 µL; detection wavelength, 210 nm; and mobile phase (methanol/water ratio, 30:70).

2.4. Measurements of the Skin Permeation Rate with Different Cosmetic Formulations

Laboskin from 7-week-old mice was thawed to room temperature and prepared using surgical scissors into a circular shape with an area of approximately 1.5 cm². Laboskin was mounted in a Franz diffusion cell with circulating water at a constant temperature of 37 °C. Then, 15 mg of a test solution (water, lotion, or emulsion) was applied to the skin. The receptor chamber was filled with approximately 10 mL of PBS and stirred with a magnetic stirrer, and 100-µL samples were collected after 2, 4, 8, 12, and 24 h. The samples were stored at −30 °C for later analysis using HPLC.

After 24 h, the skin samples were immersed overnight in 300 µL of ethyl acetate. The extract was placed in an evaporator (Tokyo Rikakikai Co. Ltd., Tokyo, Japan) to remove the solvent. Once the extract was completely dried and stored at −30 °C for later analysis, the samples were dissolved in 200 µL of methanol before analysis using HPLC. The HPLC conditions were identical to those described in Section 2.3.

2.5. Analysis of the Unknown Substance

After the samples were analyzed using HPLC, an unknown peak at 210 nm appeared on the chromatogram. To identify it, various possible substances, including RK and RD-quinone, were analyzed using HPLC. The detected absorption spectra were compared, and matching components were further verified using liquid chromatography–mass spectrometry (LC–MS).

The HPLC conditions were identical to those described in Section 2.3.

LC–MS was performed using a JMS-T100LC AccuTOF™ LC-TOFMS (JEOL DATUM Ltd., Tokyo, Japan) with Capcell Pak C18 columns (4.6 × 250 mm) at 35 °C with the following conditions: flow rate, 1.0 mL/min (approximately a quarter of the mobile phase was induced to the MS analyzer using a splitter); injection volume, 2 µL; detection wavelength, 210 nm; mobile phase (methanol/water ratio, 30:70); ionization, electrospray ionization (ESI) –; ionization voltage, –2000 V.

2.6. RK Generation by the Skin with Different Treatments

To investigate the mechanism of RK generation, a skin permeation test with the different treatments was performed, where 100-µL samples were collected after 24 h. The different experimental conditions included (1) heated skin, where laboskin was heated to 95 °C to deactivate the enzymes; (2) no skin, where laboskin was not mounted in a Franz diffusion cell and RD was added to PBS in the receptor chamber at the concentration that was in the receptor chamber after 24 h during the skin permeation test described in Section 2.4; and (3) normal laboskin as a control. The control was set as normal mouse skin. Other experimental conditions were identical to those described in Section 2.4.

2.7. Conversion of RD to RK by ADH

The reaction solutions, which comprised a 9.18-mL sodium pyrophosphate buffer (10.9 mmol/L, pH 8.8), 9 mL ADH (0, 1, 10, and 100 U/mL), 0.09 mL NAD⁺ (10 mmol/L), and 0.09 mL RD (100 mmol/L), were allowed to react at 25 °C for 30, 60, or 120 min. The RD and RK concentrations were measured using HPLC. The experiment was repeated three times.

2.8. Statistical Analysis

Numerical data were recorded in Excel (Microsoft, Redmond, WA, USA), and the means and standard deviations were calculated. The data shown in Table 2 were analyzed using two-way repeated measures analysis of variance and BellCurve Excel Statistics (Social Survey Research Information Co., Ltd., Tokyo, Japan). Tukey's test was used for multiple comparisons. For the data presented in Figure in Section 3.4, two-tailed t-tests were performed. A *p* value of <0.05 was considered statistically significant.

3. Results

3.1. Skin Permeability of RD-Containing Solutions after Repeated Application

The experimental results are shown in Figure 2. The cumulative skin penetration of RD after 8 h was 102.1 µg/cm² when applied once, 196.6 µg/cm² after 8 h when applied for a second time after 10 min, and 365.1 µg/cm² after 8 h when applied three times at 10-min intervals. The amount of penetration into the skin increased in proportion to the number of applications. Therefore, we could conclude that the concentration of RD in the skin increased with an increased number of applications.

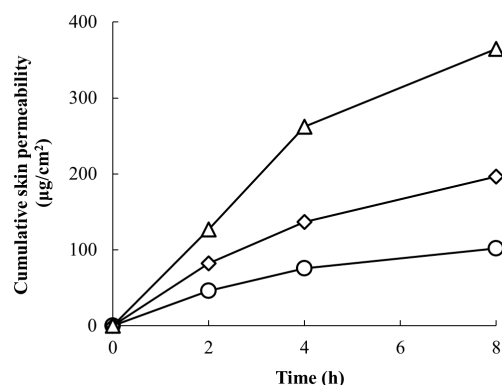


Figure 2. Repeated application of the 2% RD solution increased skin permeability (circles, ○: one application; diamonds, ◇: two applications; and triangles, △: three applications). All data points are the means of two experiments.

3.2. Skin Permeation Rates of Different Cosmetic Formulations

The skin permeation of RD in different dosage forms was studied using an in vitro skin permeation test. Samples collected after 2, 4, 8, 12, and 24 h and were quantified using HPLC. Then, the data were used to calculate the level of skin permeation, skin permeation rate, and recovery rate. After examining different types of HPLC columns, types of mobile phase, detection wavelengths, etc., the best separation analysis possible under the conditions was described in the Materials and Methods section. The recovery ratios of RD in water, lotion, and emulsion formulations are shown in Table 2. The cumulative skin permeability, permeation rate, and apparent permeability coefficient are shown in Table 3. The skin permeation amounts and skin permeation rates are shown in Figure 3.

As shown in Table 2, the recovery ratio of RD from the receptor chamber was nearly 100% for the aqueous solutions and lotions, whereas the recovery ratio of RD was about 87% for the emulsions. As shown in Table 4, there was no significant difference in the permeation ratio of RD between the water and lotion formulations or between the lotion and emulsion formulations. However, there was a significant difference in the permeation ratio of RD between the water and emulsion formulations. Therefore, the penetration rate of RD in the aqueous solution was higher than that in the lotion and emulsion formulations (Figure 3). After finite dose treatment, the permeation rate exhibited a decreasing trend over time for all formulations (Figure 3). A multiple comparisons test for differences among the formulations revealed significant differences between the water and lotion formulations and between the water and emulsion formulations after 2 h (Table 5). Significant differences were observed only between the water and emulsion formulations after 4 h. However, no significant differences among the groups were observed after 8, 12, and 24 h (Table 5).

Table 2. RD recovery rate with different cosmetic formulations.

	RD Recovery Ratio in Receptor Chamber (%)	RD Recovery Ratio in Mice Skin (%)	Total RD Recovery Ratio (%)
Water	106.6 ± 6.3	0.480 ± 0.065	107.1 ± 6.4
Lotion	100.0 ± 3.2	0.331 ± 0.210	100.3 ± 3.4
Emulsion	87.0 ± 9.1	0.408 ± 0.104	87.4 ± 9.2

Table 3. Cumulative skin permeability, permeation rate, and apparent permeability coefficient of RD with different cosmetic formulations.

	Time (h)	Cumulative Skin Permeability ($\mu\text{g}/\text{cm}^2$)	Permeation Rate ($\mu\text{g}/\text{cm}^2/\text{h}$)	Apparent Permeability Coefficient #
Water	2	40.52	20.26	0.1013
	4	65.03	12.26	0.0613
	8	97.56	8.13	0.0406
	12	127.65	7.52	0.0376
	24	213.16	7.13	0.0356
Lotion	2	28.80	14.40	0.0720
	4	47.10	9.15	0.0457
	8	86.31	9.80	0.0490
	12	121.67	8.84	0.0442
	24	200.06	6.53	0.0327
Emulsion	2	24.36	12.18	0.0609
	4	35.94	5.79	0.0289
	8	59.32	5.84	0.0292
	12	89.55	7.56	0.0378
	24	173.91	7.03	0.0351

The apparent permeability coefficient was calculated by dividing the permeation rate by the initial amount of RD ($\mu\text{g}/\text{cm}^2$) applied to the skin.

Table 4. Comparison of RD permeation rates among the formulations.

Comparison between Formulations	<i>p</i> Value
Water vs. Lotion	0.3534
Water vs. Emulsion	0.0032
Lotion vs. Emulsion	0.0877

Table 5. Multiple comparisons test to evaluate differences in the RD permeation rates among the formulations based on time after application.

Time after Application	Comparison between Formulations	<i>p</i> Value
2 h	Water vs. Lotion	0.0239
	Water vs. Emulsion	0.0016
	Lotion vs. Emulsion	0.5471
4 h	Water vs. Lotion	0.3133
	Water vs. Emulsion	0.0118
	Lotion vs. Emulsion	0.2614
8 h	Water vs. Lotion	0.7070
	Water vs. Emulsion	0.5284
	Lotion vs. Emulsion	0.1600
12 h	Water vs. Lotion	0.8068
	Water vs. Emulsion	0.9999
	Lotion vs. Emulsion	0.8158
24 h	Water vs. Lotion	0.9569
	Water vs. Emulsion	0.9988
	Lotion vs. Emulsion	0.9696

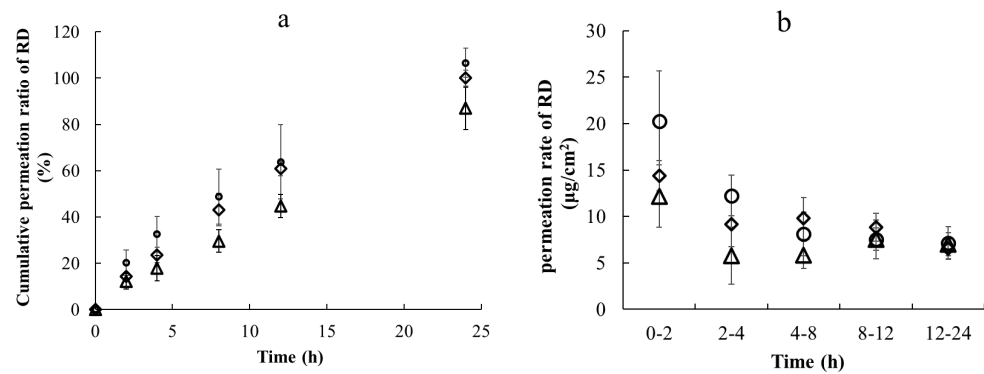


Figure 3. Cumulative rate of permeation of RD with different cosmetic formulations after different times (a) and permeation rates of RD with different cosmetic formulations in different time periods (b) under application of a 2% RD solution with a finite dose (○, water; ◇, lotion; and △, emulsion). Each point shows the mean \pm standard deviation ($n = 3$).

3.3. Analysis of the Unknown Substance

The 24-h *in vitro* skin permeation study revealed an unknown peak at 210 nm in the HPLC chromatogram (Figure 4). To identify this peak, a variety of possible substances, including RK (m.w. 164.2 kD), was analyzed using HPLC. The detected absorption spectra were compared, and the matching components were further confirmed using optimized LC–MS. As shown in Figure 4, the mass-to-charge ratio (m/z) of deprotonated anion for the authentic RK standard was 163.10 (Figure 5a). The same molecular ion peak with an m/z of 163.11 was detected in the sample (Figure 5b). Thus, LC–MS demonstrated that the unknown substance was RK.

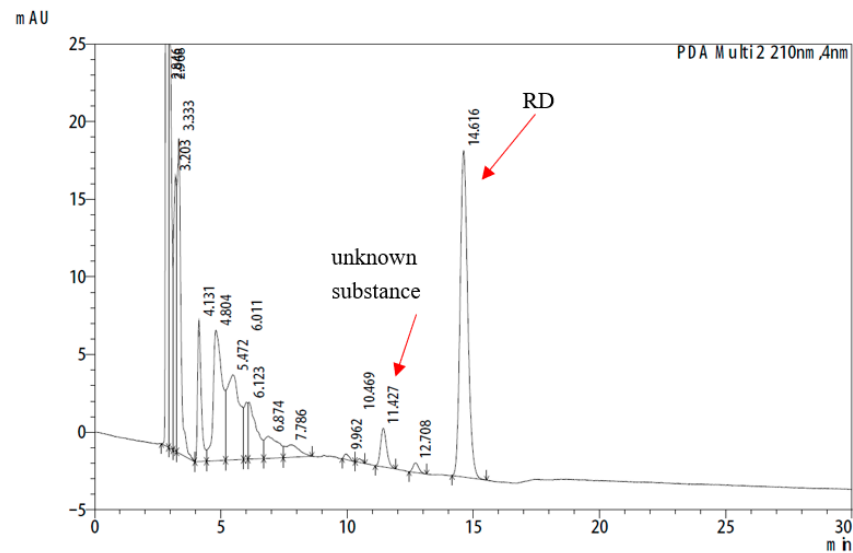


Figure 4. The unknown peak appearing at 210 nm on the HPLC chromatogram.

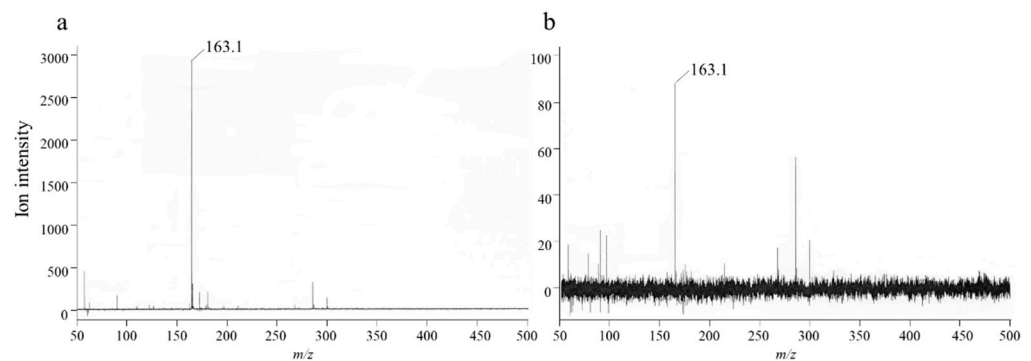


Figure 5. Mass spectra of different substances. Mass spectra of (a) RK standard and (b) RK in the sample.

3.4. RK Generation by the Skin with Different Treatments

A graph comparing the RK production after 24 h in differently treated skin is shown in Figure 6. Compared with the control, no RK production was observed in the aqueous or lotion formulations after heating the laboskin to 95 °C to deactivate the enzymes. RK production was observed in the emulsion formulation after heating the laboskin, but the amount produced was significantly lower than that in the control. No RK production was observed when the laboskin was not mounted in a Franz diffusion cell.

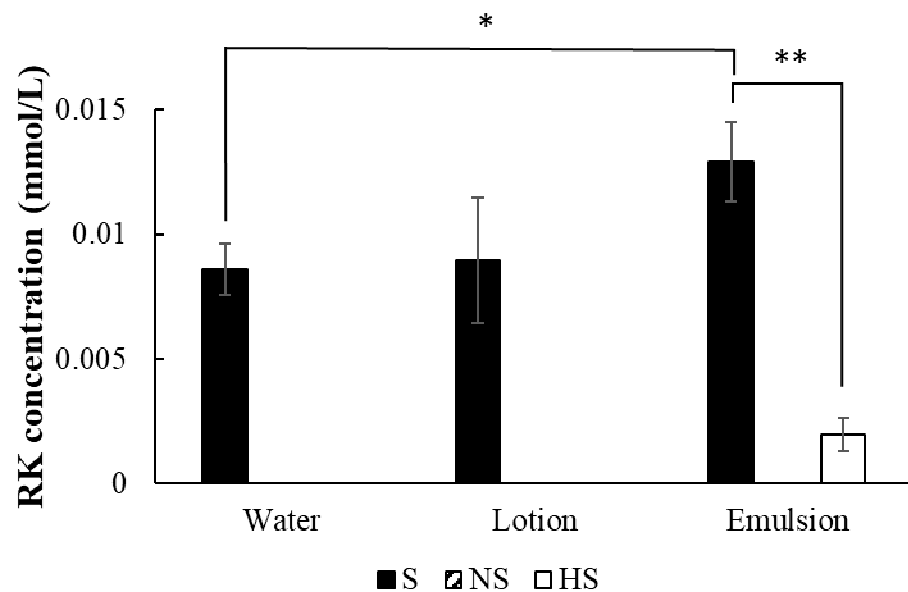


Figure 6. RK generation by the skin with different treatments. RK concentrations in 24-h samples are shown under application of a 2% RD solution with a finite dose (■, normal skin; ▨, no skin; □, heated skin). *, $p < 0.05$, emulsion formulation vs. water formulation with the same normal skin; **, $p < 0.01$, heat treatment (−) vs. heat treatment (+) with the same emulsion formulation). RK concentrations of NS (water, lotion, and emulsion) and HS (water and lotion) were below the detection limit.

3.5. Conversion of RD to RK by ADH

As shown in Figure 7, the conversion of RD to RK after 30 min was not detected in the presence of any ADH dose, whereas partial conversion of RD to RK was observed after 60 min in the presence of ADH at ≥ 9.8 units/mL. Furthermore, after 120 min, RD was converted to RK in the presence of ADH at ≥ 0.98 units/mL. These results indicated that the effect was concentration- and time-dependent.

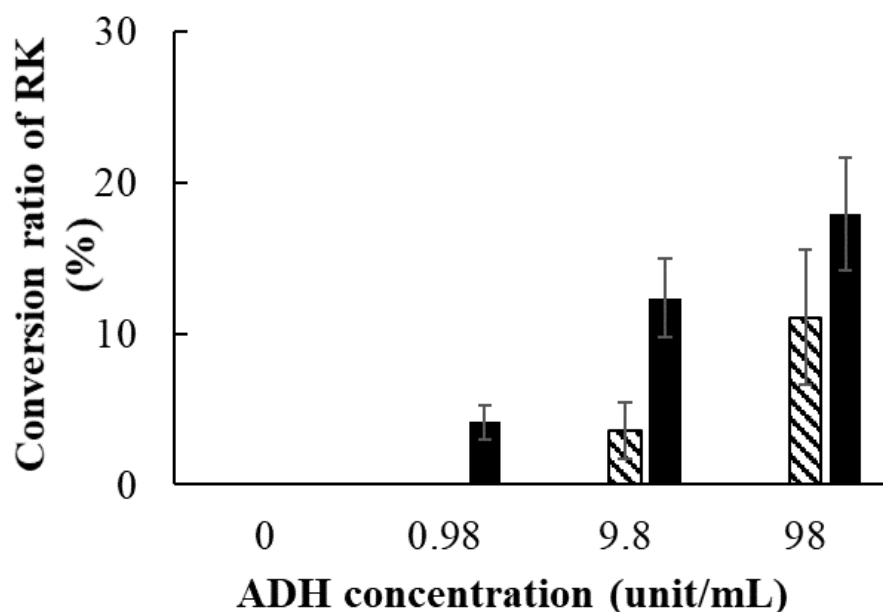


Figure 7. Conversion of RD to RK by alcohol dehydratase (ADH). The effect of different concentrations of ADH and different times on the RK conversion ratio is shown with the application of different doses of ADH (in final concentrations of 0, 0.98, 9.8, or 98 units/mL) after different times (□, 30 min; ▨, 60 min; and ■, 120 min). Data are presented as means \pm standard deviation ($n = 3$). RK concentrations after 30 min (when ADH concentrations were 0, 0.98, 9.8, and 98 units/mL) and after 60 min (when ADH concentrations were 0 and 0.98 units/mL) were below the detection limit.

4. Discussion

As the living organism's boundary, the skin is the largest organ of the human body. It possesses key enzymes found in other tissues. Topically applied substances are metabolized in the skin and converted into medicinal or toxic substances [18]. Therefore, for drugs and cosmetics that are metabolized in the skin, the potential toxicity of the metabolites should be considered.

In this study, 15 mg of a 2% RD solution was applied to 1.5 cm² of mouse skin at a dosage of 10 mg/cm². Repeated applications increased the concentration of RD in the skin, which reflected the actual usage of the product. Our tests reproduced the application of cosmetics, where the contact time with the skin was short. It is not scientifically correct to apply an infinite-volume test design, where a large amount of solution remains on the donor side, to a cosmetic product that evaporates after application. Moreover, as cosmetics, especially those aimed at brightening skin, are often applied at night before sleeping, the maximum duration for which they remain on the skin tends to exceed 8 h. Therefore, it is scientifically appropriate to evaluate the safety of brightening cosmetics over an 8-h duration. The 24-h skin permeation test using finite-volume conditions revealed that some of the RD that penetrated the skin was oxidized to RK after the application of water and cosmetic formulations (lotion and emulsion) to the full-thickness dorsal skin from hairless mice. The emulsion formulation had a higher percentage of RD oxidized to RK compared with the lotion and water formulations.

In addition, in experiments evaluating the generation of RK in laboskin exposed to different formulations, we found that any RD that did not penetrate the skin was not oxidized to RK when laboskin was not mounted in the Franz diffusion cell, even when RD was added to PBS in the receptor chamber at 37 °C. This result suggests that the oxidation of RD to RK is caused by the skin and not by the temperature. Furthermore, when the skin was heated to 95 °C to deactivate the skin enzymes, it was found that RD was not oxidized to RK in the water and lotion formulations. Some RD in the emulsion formulation was oxidized to RK, although significantly less so than in the control (normal laboskin). This implies that enzymes in the skin may be involved in the oxidation of RD to RK and

that some components in the emulsion formulation may also promote the oxidation of RD, which is supported by the fact that the oxidation ratio of RD was higher in the emulsion formulation than in the water formulation. As RK is more than twice as potent as RD in the generation of hydrogen peroxide by tyrosinase [8], the metabolism of RD to RK in the epidermis may be one of the mechanisms leading to increased susceptibility to leukoderma caused by cosmetics containing RD.

Some previous studies have suggested that RK has a risk of causing leukoderma [9,10,19]. According to a 1998 study, three workers engaged in RK production suffered from leukoderma, and two of them were not completely cured [8–10]. RD-induced leukoderma appears to be due to the catalysis of tyrosinase, generating o-quinone, which results in oxidative stress and cell toxicity. RK-induced leukoderma appears to be due to the destruction of melanocytes by a toxic substance produced by the action of tyrosinase on RK [20]. The metabolism from RD to RK, which is considered to be related to leukoderma, may also be another cause of leukoderma. It has been reported that (R)-RD [19,21] in plants is converted to RK by ADH [22]. As ADH is a ubiquitously expressed enzyme that is also present in human skin [23], it is possible that RD, a secondary alcohol, is oxidized to RK. It has also been reported that the yeast *Candida boidinii* transforms (R)-RD into RK [24]. Thus, RD and RK are very similar compounds in terms of chemical structure and metabolic biosynthesis. Therefore, we investigated whether RD was converted to RK by ADH and confirmed that RD was converted to RK by ADH at a level of 0.98 units/mL (3.27 nmol/mg protein/min) or higher. The reported ADH activity in the skin was 0.32–0.41 nmol/mg protein/min in humans [25], indicating that RD is converted to RK by ADH in human skin.

Regarding the oxidative stability of the R- and S-enantiomers of secondary alcohols, it was reported that when a racemic mixture of secondary alcohols was added to the cultured cells of *Catharanthus roseus*, the S-enantiomer of the racemic mixture was rapidly oxidized to the ketone form; however, it was immediately asymmetrically reduced to the R-enantiomer without being isolated, whereas the R-enantiomer was stable against the oxidation reaction [26]. There are many reports that the R- and S-enantiomers have different effects. For example, thalidomide was synthesized as a racemic mixture of equal amounts of R- and S-enantiomers. It was later reported that the R-enantiomer was harmless, but the S-enantiomer was highly teratogenic and caused fetal abnormalities [27–29]. Ibuprofen is active only in the S-enantiomer; the R-enantiomer is converted to the S-enantiomer by enzymatic action in vivo [30,31]. These examples suggest the possibility that the S-enantiomer is more potent and toxic compared with the R-enantiomer. Therefore, chemically synthesized racemic mixtures should be thoroughly tested and carefully examined.

The R- and S-enantiomers of RD, which are potential substrates for tyrosinase, differ in the strengths of their effects and side effects; the S-enantiomer is expected to have stronger effects and side effects. It was expected from the beginning of the development of cosmetics containing RD that if a product containing a 2% racemic mixture of RD is applied, and if the R-enantiomer is easily isomerized to the S-enantiomer in the skin, the effects and side effects of the product will be enhanced.

This experiment was conducted with a racemic mixture. It was not possible to clarify whether the R- or S-enantiomer of RD was converted to RK, both enantiomers were converted, or there was a difference in the degree of conversion. As there are technologies to synthesize the R- and S-enantiomers of RD separately [32] and to split them [33,34], future tests should be conducted with separated R- and S-enantiomers.

5. Conclusions

This study further clarifies the mechanisms of RD-induced leukoderma. RD is partially metabolized to RK after its absorption in the cornified layer, with enzymes in the skin appearing to be the cause. One such enzyme was found to be ADH. The intraepidermal oxidation of RD to RK may be one of the mechanisms of RD-induced susceptibility to leukoderma. Furthermore, the cosmetic ingredients of the emulsion formulation may promote the oxidation of RD to RK.

Author Contributions: Conceptualization, L.G. and K.M.; methodology, L.G. and K.M.; validation, L.G. and A.F.; formal analysis, L.G. and A.F.; investigation, L.G. and A.F.; data curation, L.G. and K.M.; writing—original draft preparation, L.G.; writing—review and editing, K.M.; visualization, L.G.; supervision, K.M. All authors have read and agreed to the published version of the manuscript.

Funding: This research received no external funding.

Institutional Review Board Statement: Not applicable.

Informed Consent Statement: Not applicable.

Data Availability Statement: Not applicable.

Acknowledgments: We would like to thank Tomomi Takahashi for his help in the preliminary experiments on determining RD concentrations in the skin after repeated RD applications.

Conflicts of Interest: The authors declare no conflict of interest.

References

1. Maeda, K. Advances in development of skin whitening agents. *Fragr. J.* **2008**, *36*, 65–67. (In Japanese)
2. Homepage of Kanebo Cosmetics, Inc. The Number of Checks of the White Spots' Condition, and Recovery, a Reconciliation Situation/the Number of Object Recall. Available online: http://www.kanebo-cosmetics.jp/information/correspondence/data_2016.html (accessed on 25 August 2021).
3. Ito, S.; Okura, M.; Nakanishi, Y.; Ojika, M.; Wakamatsu, K.; Yamashita, T. Tyrosinase-catalyzed metabolism of rhododendrol (RD) in B16 melanoma cells: Production of RD-pheomelanin and covalent binding with thiol proteins. *Pigment Cell Melanoma Res.* **2015**, *28*, 295–306. [[CrossRef](#)] [[PubMed](#)]
4. Sasaki, M.; Kondo, M.; Sato, K.; Umeda, M.; Kawabata, K.; Takahashi, Y.; Suzuki, T.; Matsunaga, K.; Inoue, S. Rhododendrol, a depigmentation-inducing phenolic compound, exerts melanocyte cytotoxicity via a tyrosinase-dependent mechanism. *Pigment Cell Melanoma Res.* **2014**, *27*, 754–763. [[CrossRef](#)] [[PubMed](#)]
5. Ito, S.; Okura, M.; Wakamatsu, K.; Yamashita, T. The potent pro-oxidant activity of rhododendrol–eumelanin induces cysteine depletion in B16 melanoma cells. *Pigment Cell Melanoma Res.* **2017**, *30*, 63–67. [[CrossRef](#)] [[PubMed](#)]
6. Tokura, Y.; Fujiyama, T.; Ikeya, S.; Tatsuno, K.; Aoshima, M.; Kasuya, A.; Ito, T. Biochemical, cytological, and immunological mechanisms of rhododendrol-induced leukoderma. *J. Dermatol. Sci.* **2015**, *77*, 146–149. [[CrossRef](#)]
7. Ito, S.; Wakamatsu, K. A convenient screening method to differentiate phenolic skin whitening tyrosinase inhibitors from leukoderma-inducing phenols. *J. Dermatol. Sci.* **2015**, *80*, 18–24. [[CrossRef](#)]
8. Gu, L.; Zeng, H.; Takahashi, T.; Maeda, K. In vitro methods for predicting chemical leukoderma caused by quasi-drug cosmetics. *Cosmetics* **2017**, *4*, 31. [[CrossRef](#)]
9. Fukuda, Y.; Nagano, M.; Futatsuka, M. Occupational leukoderma in workers engaged in 4-(p-hydroxyphenyl)-2-butanone manufacturing. *J. Occup. Health* **1998**, *40*, 118–122. [[CrossRef](#)]
10. Fukuda, Y.; Nagano, M.; Tsukamoto, K.; Futatsuka, M. In vitro studies on the depigmenting activity of 4-(p-hydroxyphenyl)-2-butanone. *J. Occup. Health* **1998**, *40*, 137–142. [[CrossRef](#)]
11. Okmura, Y.; Shirai, T. Vitiliginous lesions occurring among workers in a phenol derivative factory. *Jpn. J. Dermatol.* **1962**, *7*, 617–619.
12. James, O.; Mayes, R.W.; Stevenson, C.J. Occupational vitiligo induced by *p*-tert-butylphenol, a systemic disease? *Lancet* **1977**, *2*, 1217–1219. [[CrossRef](#)]
13. Ebner, H.; Helletzgruber, M.; Höfer, R.; Kolbe, H.; Weissel, M.; Winker, N. Vitiligo from *p*-tert. butylphenol; A contribution to the problem of the internal manifestations of this occupational disease. *Dermatosen Beruf Umw.* **1979**, *27*, 99–104.
14. Budde, J.; Stary, A. Skin and systemic disease caused by occupational contact with *p*-tert-butylphenol. Case reports. *Dermatosen Beruf Umw.* **1988**, *36*, 17–19.
15. Rodermund, O.E.; Jörgens, H.; Müller, R.; Marsteller, H.J. Systemic changes in occupational vitiligo. *Hautarzt* **1975**, *26*, 312–316. [[PubMed](#)]
16. Ikeda, M.; Ohtsuji, H.; Miyahara, S. Two cases of leucoderma, presumably due to nonyl or octylphenol in synthetic detergents. *Ind. Health* **1970**, *8*, 192–196. [[CrossRef](#)]
17. Russell, O.; Richard, H. Predicting skin permeability. *Pharm. Res.* **1992**, *9*, 663–669.
18. Hisatomi, A.; Kimura, M.; Maeda, M.; Matsumoto, M.; Ohara, K.; Noguchi, H. Toxicity of polyoxyethylene hydrogenated castor oil 60 (HCO-60) in experimental animals. *J. Toxicol. Sci.* **1993**, *18*, 1–9. [[CrossRef](#)] [[PubMed](#)]
19. Reddy, P.S.; Jamil, K.; Madhusudhan, P.; Anjani, G.; Das, B. Antibacterial activity of isolates from piper longum and *Taxus baccata*. *Pharm. Biol.* **2001**, *39*, 236–238. [[CrossRef](#)]
20. Ito, S.; Hinoshita, M.; Suzuki, E.; Ojika, M.; Wakamatsu, K. Tyrosinase-catalyzed oxidation of the leukoderma-inducing agent raspberry ketone produces (*E*)-4-(3-oxo-1-butenyl)-1,2-benzoquinone: Implications for melanocyte toxicity. *Chem. Res. Toxicol.* **2017**, *30*, 859–868. [[CrossRef](#)]

21. Parmar, V.S.; Vardhan, A.; Taneja, P.; Sinha, R.; Patnaik, G.K.; Tripathi, S.C.; Boll, P.M.; Larsen, S. Absolute configuration of epi-rhododendrin and (–)-rhododendrol [= (–)-betuligenol] and X-ray crystal and molecular structure of rhododendrin [= betuloside], a hepatoprotective constituent of *Taxus baccata*. *J. Chem. Soc. Perkin Trans.* **1991**, *1*, 2687–2690. [[CrossRef](#)]
22. Becker, A.; Böttcher, D.; Katzer, W.; Siems, K.; Müller-Kuhr, L.; Bornscheuer, U.T. An ADH toolbox for raspberry ketone production from natural resources via a biocatalytic cascade. *Appl. Microbiol. Biotechnol.* **2021**, *105*, 4189–4197. [[CrossRef](#)] [[PubMed](#)]
23. Pyo, S.M.; Maibach, H.I. Skin metabolism: Relevance of skin enzymes for rational drug design. *Skin Pharmacol. Physiol.* **2019**, *32*, 283–294. [[CrossRef](#)] [[PubMed](#)]
24. Fronza, G.; Fuganti, C.; Pedrocchi-Fantoni, G.; Serra, S.; Zucchi, G.; Fauhl, C.; Guillou, C.; Reniero, F. Stable isotope characterization of raspberry ketone extracted from *Taxus baccata* and obtained by oxidation of the accompanying alcohol (Betuligenol). *J. Agric. Food Chem.* **1999**, *47*, 1150–1155. [[CrossRef](#)] [[PubMed](#)]
25. Cheung, C.; Davies, N.G.; Hoog, J.O.; Hotchkiss, S.A.M.; Pease, C.K.S. Species variations in cutaneous alcohol dehydrogenases and aldehyde dehydrogenases may impact on toxicological assessments of alcohols and aldehydes. *Toxicology* **2003**, *184*, 97–112. [[CrossRef](#)]
26. Takemoto, M.; Achiwa, K. Deracemization of the racemic 4-pyridyl-1-ethanol by *Catharanthus roseus* cell cultures. *Phytochemistry* **1998**, *49*, 1627–1629. [[CrossRef](#)]
27. Blaschke, G.; Kraft, H.P.; Fickentscher, K.; Köhler, F. Chromatographic separation of racemic thalidomide and teratogenic activity of its enantiomers. *Arzneimittelforschung* **1979**, *29*, 1640–1642. [[PubMed](#)]
28. Tokunaga, E.; Yamamoto, T.; Ito, E.; Shibata, N. Understanding the thalidomide chirality in biological processes by the self-disproportionation of enantiomers. *Sci. Rep.* **2018**, *8*, 17131. [[CrossRef](#)]
29. Jacques, V.; Czarnik, A.W.; Judge, T.M.; Van der Ploeg, L.H.; DeWitt, S.H. Differentiation of antiinflammatory and antitumorigenic properties of stabilized enantiomers of thalidomide analogs. *Proc. Natl. Acad. Sci. USA* **2015**, *112*, E1471–E1479. [[CrossRef](#)]
30. Kaiser, D.G.; Vangiessen, G.J.; Reischer, R.J.; Wechter, W.J. Isomeric inversion of ibuprofen (R)-enantiomer in humans. *J. Pharm. Sci.* **1976**, *65*, 269–273. [[CrossRef](#)]
31. Ikuta, H.; Kawase, A.; Iwaki, M. Stereoselective pharmacokinetics and chiral inversion of ibuprofen in adjuvant-induced arthritic rats. *Drug Metab. Dispos.* **2017**, *45*, 316–324. [[CrossRef](#)]
32. Sabitha, G.; Thirupathaiyah, B.; Yadav, J.S. Asymmetric synthesis of (R)-(-)-rhododendrol, the aglycone of the hepatoprotective agent rhododendron. *Synth. Commun.* **2007**, *37*, 1683–1688. [[CrossRef](#)]
33. Yuasa, Y.; Shibuya, S.; Yuasa, Y. Resolution of racemic rhododendrol by lipase-catalyzed enantioselective acetylation. *Synth. Commun.* **2003**, *33*, 1469–1475. [[CrossRef](#)]
34. Karume, I.; Takahashi, M.; Hamdan, S.M.; Musa, M.M. Deracemization of secondary alcohols by using a single alcohol dehydrogenase. *ChemCatChem* **2016**, *8*, 1459–1463. [[CrossRef](#)]